REPORTS OF THE SWEDISH DEEP-SEA EXPEDITION. VOL. III
PHYSICS AND CHEMISTRY. NO. 5

# THE EQUATORIAL CURRENTS IN THE INDIAN OCEAN

BY

N. G. JERLOV

The Equatorial Currents in the Indian Ocean show great seasonal variations. Only the South Equatorial Current is permanent throughout the year, which is due to the south-east trade wind. The North Equatorial Current is maintained by the north-east monsoon blowing during the northern winter. Between these two currents, flowing toward the west, the Countercurrent, which is present south of the Equator, is well developed during February and March.

According to programme the Swedish Deep Sea Expedition was to make an investigation of the Countercurrent in the Indian Ocean which so far had not been studied in detail from an oceanographic point of view. Our intention was to cross the system of Equatorial Currents at least by one section in the central part of the equatorial region, which area up to that time had not been covered by any of the modern oceanographic expeditions. The *Albatross* after unavoidable delay — partly due to stormy weather south of Bali — started its work in the Indian Ocean at the end of February. During the first half of March the planned section across the Equatorial Currents was run from 11° S to 2° N near long. 88° E. Seven stations with serial observations (Stations 200—208) were taken in the section. A second section with seven stations between Ceylon and the Seychelles could not, as had been our intention, be extended over the Equatorial Currents. Time was short, as the *Albatross* must necessarily leave the Indian Ocean before the south-west monsoon began to blow.

The surface currents in the Indian Ocean have been treated on the basis of old data by Lotte Möller (1929). Since then, the *Dana*, the *Discovery*, the *Snellius* expeditions, and the »John Murray Expedition» have contributed to the oceanographic exploration mainly of the western and eastern parts of the equatorial region. Our present knowledge of the equatorial surface currents is set out on charts published by Schott (1943). These charts show that during the northern winter the position of the southern boundary of the Countercurrent varies very little in a zonal direction from 7° to 8° S. Off the African coast the northern boundary falls near 4° S. Here the Countercurrent reaches maximum strength fed by the South Equatorial Current which turns north at 10° S. Towards the east the Countercurrent broadens and the northern boundary gradually moves towards the Equator.

## Horizontal Distribution of Temperature, Salinity and Density

Figs. 1—5 have been prepared to show the actual course of the isopleths at our stations with due regard to the charts by Schott (1935) in areas where *Albatross* data are lacking. The horizontal distribution of properties at the surface is influenced by heating and cooling, evaporation and precipitation, temporary winds, currents etc. In consequence, the data collected by serial and surface observations from the *Albatross* are not likely to agree in all

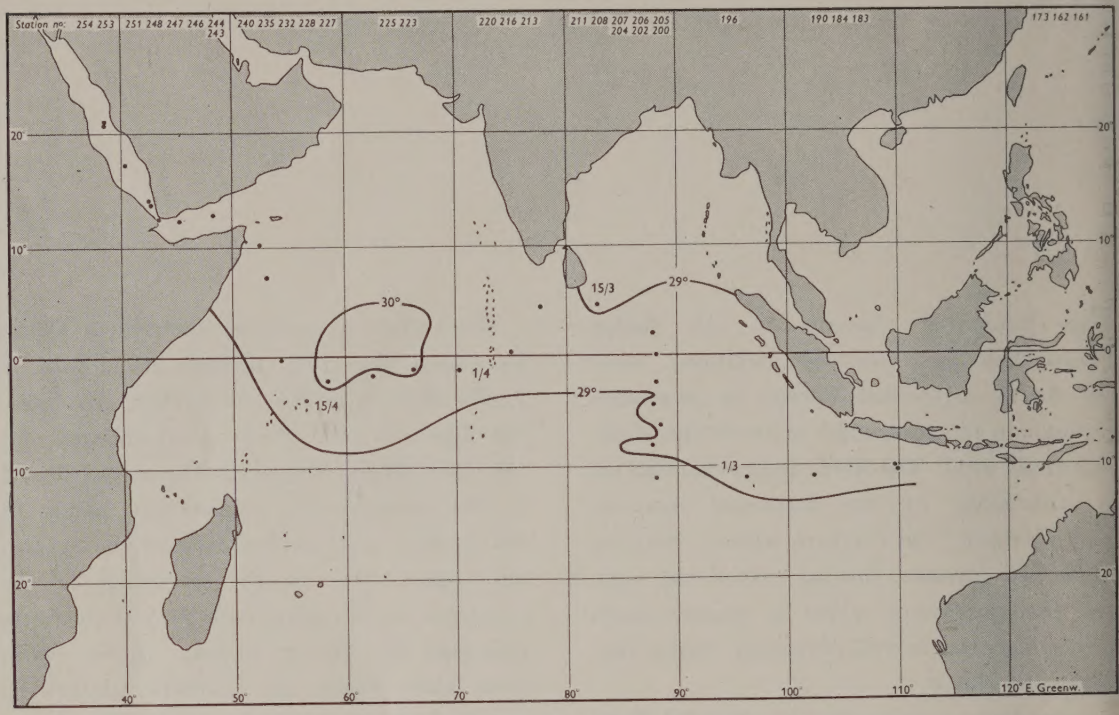


Fig. 1. Horizontal distribution of temperature at surface.

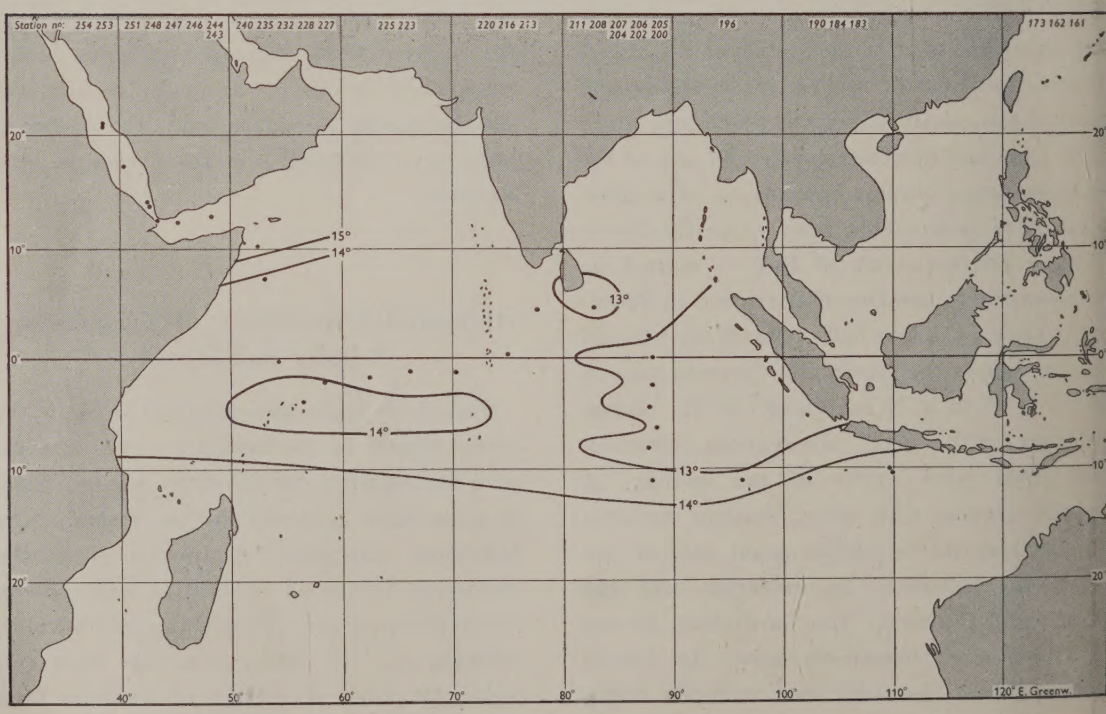


Fig. 2. Horizontal distribution of temperature at 200 m.

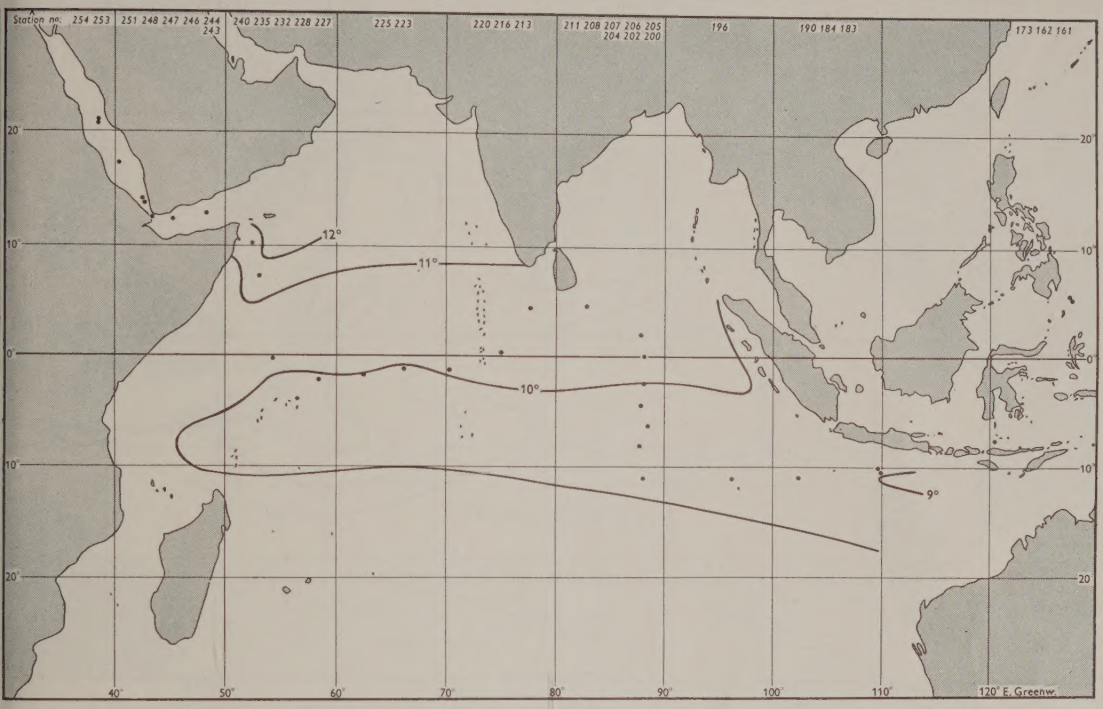


Fig. 3. Horizontal distribution of temperature at 400 m.

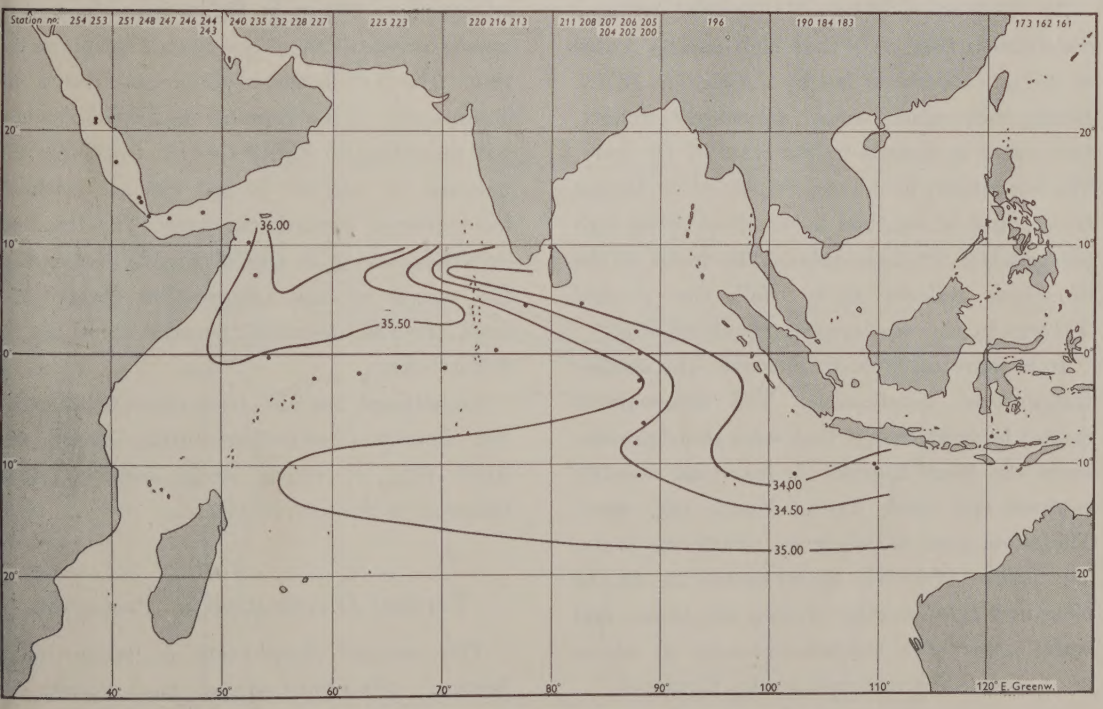


Fig. 4. Horizontal distribution of salinity at surface.

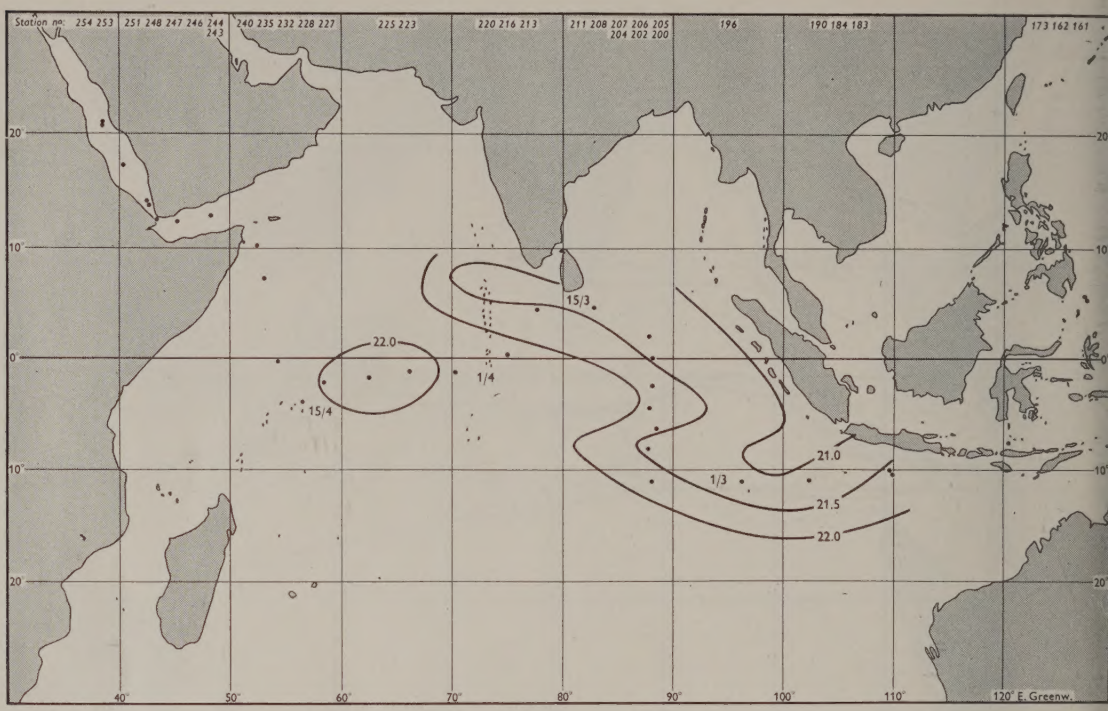


Fig. 5. Horizontal distribution of density at surface.

details with the Schott charts which represent mean annual conditions.

An outstanding feature of the surface salinity distribution (Fig. 4) is that high-salinity water of 35 $^0/_{00}$ extends as far to the east as 89° E. During the northern winter, according to Schott, this water is present to the west of 78° only. The low salinity in the eastern part of the Indian Ocean must be ascribed to the effect of the high precipitation in these areas. The trend of the isohalines reflects fairly well the general features in the equatorial current pattern.

It is more difficult to illustrate the surface temperature distribution. The observations cannot be treated as if they were simultaneous, since the Heat Equator is marching steadily towards the north during March and April. Therefore, some dates are set out on the route. The surface layer was much heated due to the clear and calm weather during the cruise, and water areas of a temperature near or above 30° C. were encountered at the Equator.

On the other hand, the temperature distribution at 200 m and 400 m is more stable and shows small seasonal variations. Comparing isotherms at 200 m in Fig. 2 with the annual values by Schott we notice a considerable deviation. The 14° isotherm dominates the whole ocean south of the Equator on the Schott chart but according to Fig. 2 the 13° isotherm runs between 80° and 90° E and the 14° isotherm has retreated towards the west. The temperature distribution at 400 m (Fig. 3) reveals that the tongue of low temperature (below 10° from the east is much broader than on the Schott chart.

An attempt has also been made to illustrate the density distribution during March and April (Fig. 5) which brings out the major features in the current system.

## Vertical Distribution of Properties

The vertical distribution of properties in Section 200—208 across the system of Equatorial Currents is presented in Figs. 6—10

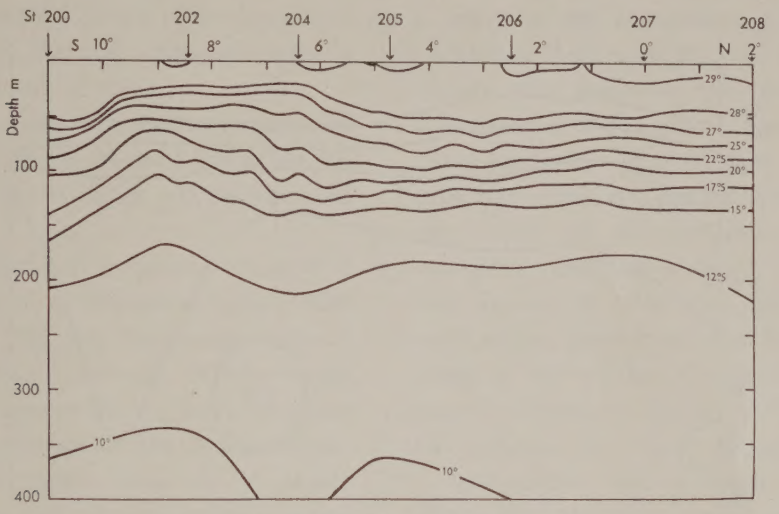


Fig. 6. Temperature.

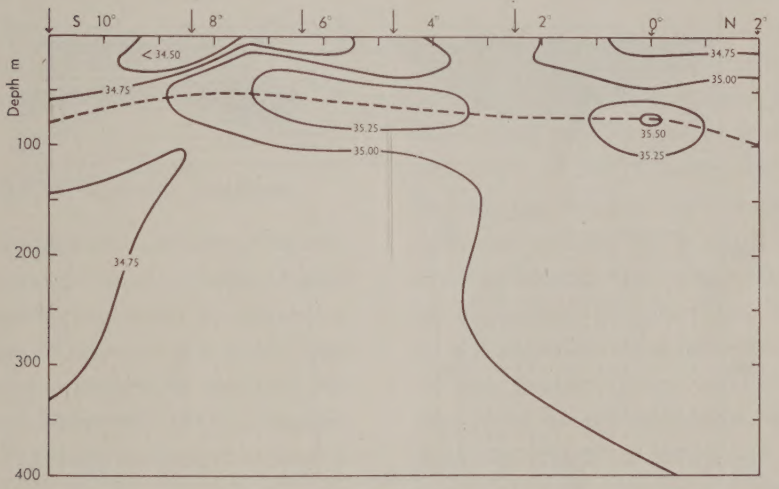


Fig. 7. Salinity.

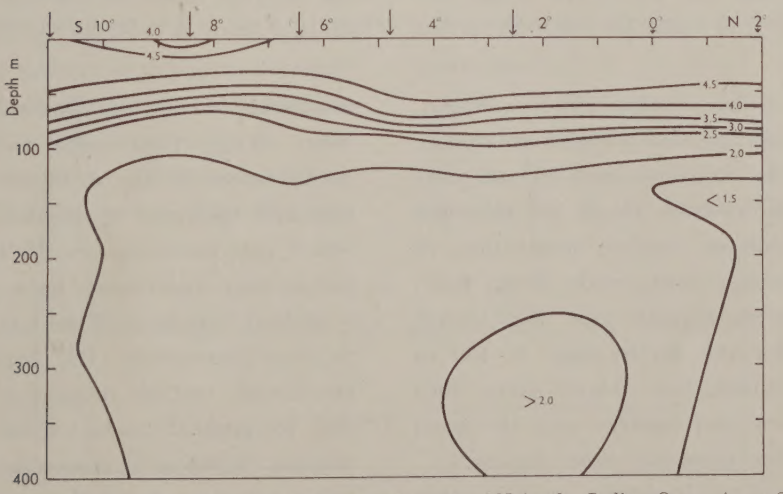


Fig. 8. Oxygen in a vertical section between 11° S and 2° N in the Indian Ocean (near 88° E).

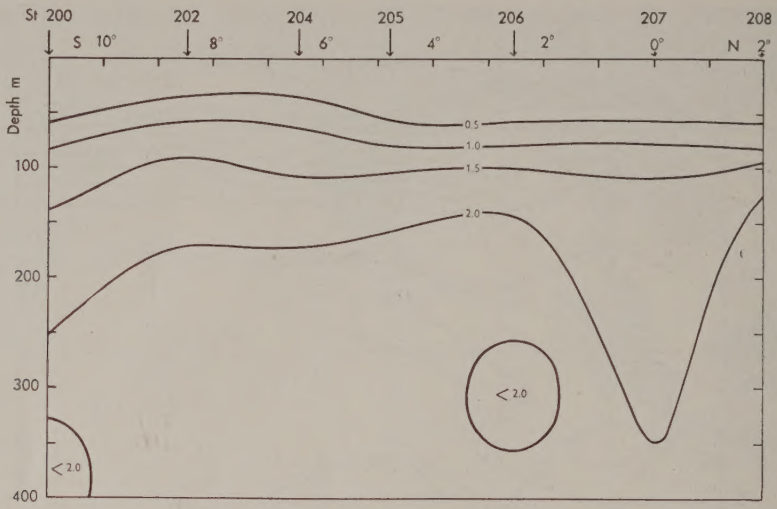


Fig. 9. Phosphate.

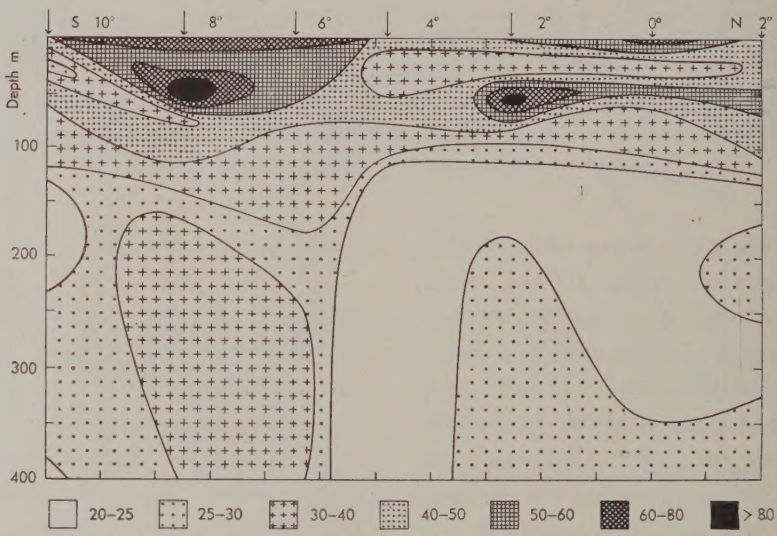


Fig. 10. Distribution of particles in a vertical section between 11° S and 2° N in the Indian Ocean (near 88° E).

Distributions of temperature, salinity, oxygen, phosphate, and suspended particles are shown. Other properties also measured do not yield any further information about the structure of the water masses. Surface observations of temperature and salinity made every hour, *i. e.* about every seventh mile, and bathythermogram for the depth range 0—130 m taken every fourth hour (about every 30th mile) have been used together with the serial observations for preparing these figures.

The trend of the isopleths in the section establishes some variations with depth. Th depth to the thermocline varies moderatel as illustrated in Fig. 6. Station 204 displa maximal thickness of the discontinuity laye which gets less thick towards the north. Th temperature distribution between the station is derived from bathythermograms and subjec to some uncertainty. But it gives an idea o the actual vertical movement in the ocea due to internal waves which produce con tinuous variations in properties at the differen levels, in particular within the discontinuity

The semidiurnal tidal period is clearly noticed as a superposed vertical oscillation with a maximal amplitude of 10 m.

The significant subsurface salinity maximum is present at all stations (dashed line in Fig. 7). The variations in its depth will be discussed later.

The salient rise of all isopleths at about 8° S gives evidence of a divergence region. The general theory for the Equatorial Currents (SVERDRUP, 1932; DEFANT, 1936 b) would claim a divergence at the southern boundary of the Countercurrent in the Indian Ocean. The divergence region being rich in phytoplankton is also well reflected in the distribution of particles shown in Fig. 10.

For the rest, the course of the isopleths does not give any sure indication about the vertical water movements.

## Topography of Isobaric Surfaces

Values of temperature, salinity, density, and computed anomalies of dynamic height at standard depths are listed in Appendix, Table 2. In order to arrive at a representation of the absolute topography of the different isobaric surfaces, DEFANT's (1941) procedure was employed. Reference surfaces of no motion have been selected for the various stations.

Proceeding from one station to the next the slope of the isobaric surfaces is found relative to the reference surface. A complete representation of the topography of the isobaric surfaces is not possible in the Equator region. The observations in the Countercurrent are too few, being confined to the section 200—208. But a profile of the absolute topography of the sea surface is given in Fig. 11. The trough at station 202 indicates the well developed divergence at the southern boundary of the Countercurrent. The slope of the surface between Stations 204 and 207 is small and does not admit of any definitive conclusions, considering that the effect of internal waves may amount to three dyn. cm. Conditions north of the Equator are more clear. There is reason to believe that the rise of the surface from the Equator to Station 208 is not illusory but indicates the North Equatorial Current.

MONTGOMERY and PALMÉN (1940) have shown that the wind stress exerted on the sea surface of the South Equatorial Current in the Pacific leads to a piling up of light surface water in the western part of the ocean. They have studied this effect by using *Dana* observations at the Equator where the deflecting force vanishes. At our Equator Stations 207, 216 and 232 the westward wind stress was low. In consequence, they show small deviations in dynamic height; Station 216 is only some dyn. cm higher than the other two. Unfortunately, no oceanographic data from the western areas of the Indian Ocean exist which can be considered as representative for the normal mass distribution in March and which can be compared with the data from our Section 200—208. Therefore, the zonal topography south of the Equator is not at present attainable.

There is however, no great objection to comparing conditions below 200 m at Station 200 (88° 26′ E, 11° 01′ S) and at *Dana* Station 3928 (50° 10′ E, 11° 20′ S). The surface $\sigma_t =$

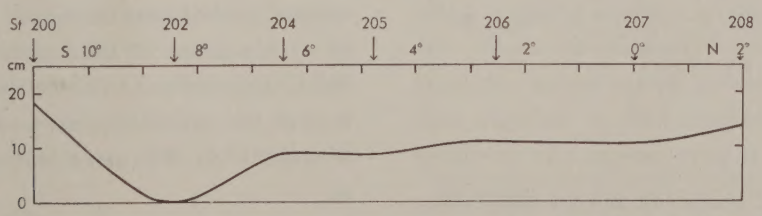


Fig. 11. Profile of the absolute topography of the sea surface between 11° S and 2° N in the Indian Ocean (near 88° E).

26.4 is in the former case found at 260 m, in the latter at 290 m. Montgomery and Palmén have found that the axial pressure gradient at Equator in the Pacific and in the Atlantic Ocean maintained by the trade wind extends to about $\sigma_t = 26.4$. It appears that this surface is practically level in the South Equatorial Current in all three oceans. It coincides roughly with the bottom of the discontinuity layer defined as the depth where the change in $\sigma_t = 0.005$ per m.

## Currents

The current velocity field, which is associated with the distribution of mass, gives a clear picture only south of 5° S. Nearer the Equator the computation of velocity is very uncertain owing to the weak Coriolis force. A profile of the distribution of computed horizontal velocity is shown in Fig. 12. The South Equatorial Current flows with a velocity of 30 cm/sec. or 0.6 knots. The surface velocity of the Countercurrent is determined at 22 cm/sec. or 0.4 knots which is an accordance with the normal value by Schott. Due to a slight headwind the Countercurrent, however, attains its maximal strength at 75 m depth. The main flow is between 6° and 8.5° S and thus comprises less than 300 km. The Schott chart for February places the northern boundary of the Countercurrent in close proximity to the Equator. In Fig. 12 a westgoing current appears between Stations 204 and 205 and an eastgoing between Stations 205 and 206. The

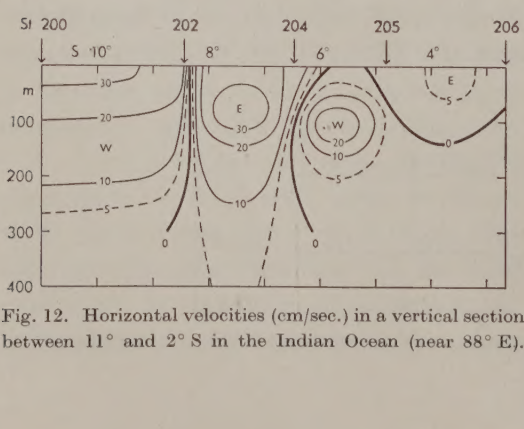


Fig. 12. Horizontal velocities (cm/sec.) in a vertical section between 11° and 2° S in the Indian Ocean (near 88° E).

reality of the latter flow, which constitutes a northern branch of the Countercurrent, is doubtful.

It may also be mentioned that between the Equator and 2° N the flow of the North Equatorial Current is suggested by the topography of the sea surface (Fig. 11).

The general feature of water transport in the system of equatorial currents in the Pacific can be accounted for by the average wind stress exerted by the prevailing winds ( Sverdrup 1947; Reid, 1948). The present material from the Indian Ocean is not suitable for a similar treatment as wind stresses are weak in the region near the Equator.

It may be added that the wind distribution recorded on board the *Albatross* was fairly normal for the season. Between Stations 200 and 202 the wind observed blew on an average with 7 m/sec. from ESE, but further north it was only 2 m/sec. from NE and soon died away. The north-east monsoon when passing the Equator generally turns north or north-west. Between Stations 207 and 208 we even met with a light wind blowing from WNW.

According to Schott, the Countercurrent bends south at about 100° E and follows the coast of Java, its southern boundary not crossing 10° S until at 115° E. However, the dynamic computation reveals a southerly component though only of 4.5 dyn. cm between Stations 183, 184 and 190 which suggets that the actual flow of the Countercurrent was more towards the south-west. Though the wind was normal in this area, WSW 5 m/sec. the distribution noted might be temporary or due to the disturbing effect of internal waves.

Our examination of the horizontal and vertical distribution of current velocities aims at a calculation of the volume transport by the Countercurrent. As mentioned, the main flow of the Countercurrent was found between 6° and 8.5° S. The magnitude of this transport is

15 million $m^3$/sec.

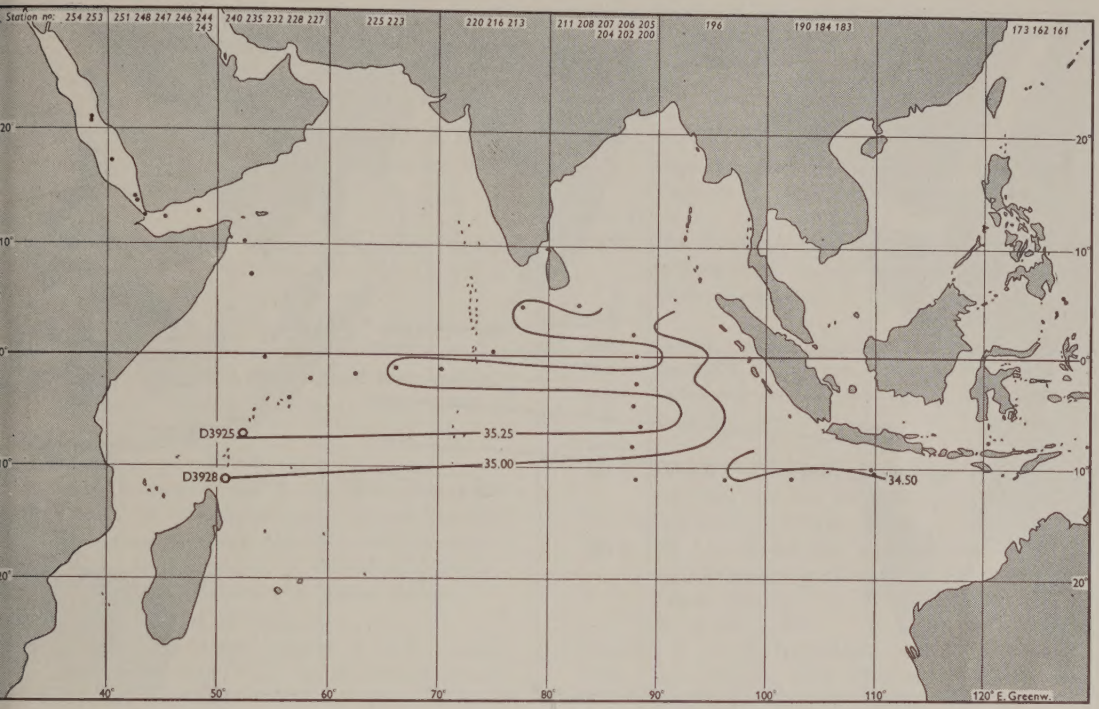


Fig. 13. Isohalines in the $\sigma_t = 23.3$ surface.

Many objections have been raised to the use of dynamic methods which do not always apply to actual conditions in nature (see *e.g.* Parr, 1938; Clowes, 1950). It is emphasized that a discussion of currents must also be based on a close study of the characteristics of the water masses. The Montgomery method (1939) of examining an identifying property along $\sigma_t$ surfaces, which are considered as quasi-isentropic surfaces in the ocean, provides another alternative for illustrating the subsurface currents.

The subsurface salinity maximum shown in Fig. 7 is present near the upper limit of the thermocline and approximately coincides with the surface $\sigma_t = 23.3$. Isohalines in this surface have been drawn on the chart in Fig. 13. Two Dana Stations, 3925 (7° 13′ S, 52° 22′ E) and the above-mentioned 3928 (11° 20′ S, 70° 10′ E) have been added to the net of *Albatross* observations, and they fit well into the pattern in Fig. 13.

The chart clearly illustrates the outlines of the water movements within the discontinuity layer. Apparently the Countercurrent is wider in this picture than in Fig. 12. At the Equator an area of maximum salinity is present, but, owing to the lack of data from the region just north of the Equator at long. 70° E, the trend of the $35.25\,^0/_{00}$ isohaline is uncertain.

Most stations in the considered region of the Equatorial Indian Ocean display another salinity maximum, usually at 350—450 m depth, which is due to the Central Water and nearly coincides with the surface $\sigma_t = 26.9$. Isohalines in this surface are shown on the chart in Fig. 14. The two Dana Stations 3925 nad 3928 are included in the figure. The isohalines run in a nearly east-west direction which suggests that the spreading of the Central Water is induced by the Equatorial currents. According to the computed dynamic data the flow in the Countercurrent attains a velocity of 5 cm/sec. even at 400 m.

Summing up, we may say that the Equatorial Currents in the Indian Ocean extend at least

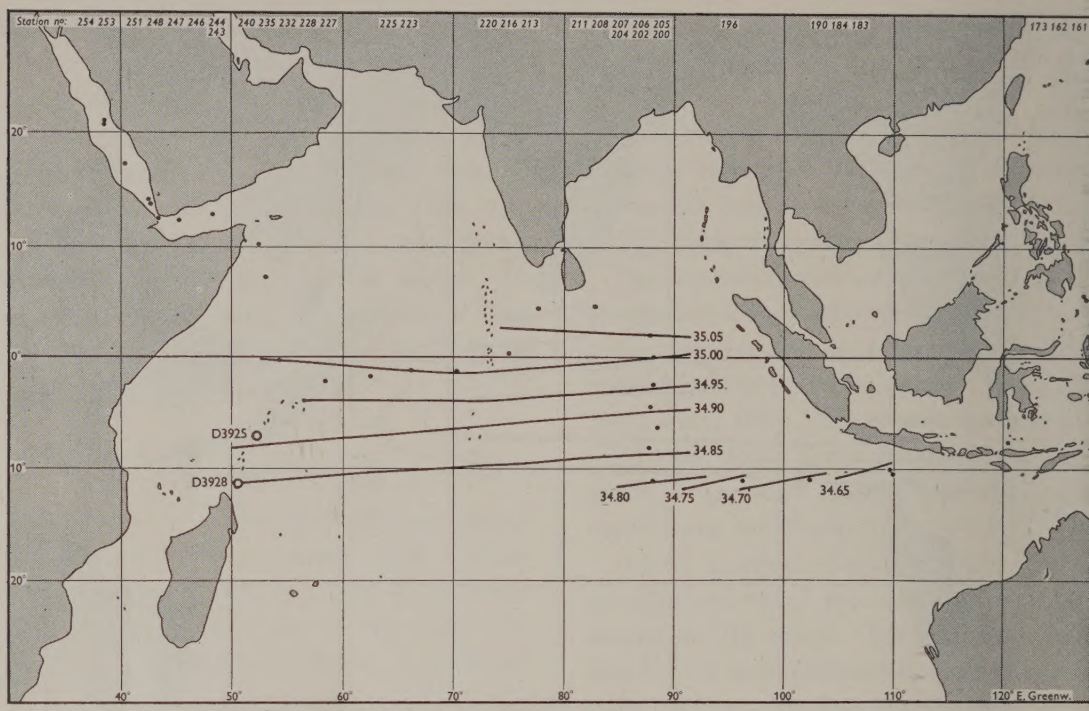


Fig. 14. Isohalines in the $\sigma_t = 26.9$ surface.

down to the bottom of the discontinuity layer as defined above, or to 200—300 m, the Countercurrent even to greater depths.

As regards the area of Stations 183—200, SVERDRUP *et al.* (1942) mention that the low-salinity water of temperature higher than 10° is probably of Pacific origin. The close packing of isohalines in Fig. 14 actually shows the presence of a new water mass at 400 m. This question, however, is beyond the scope of this report.

The examination of the Equatorial Currents in the Indian Ocean made in this report does not deal with all phases of the problem. A theoretical interpretation requires a broad basis of experimental data. The found curre pattern lacks well-developed features in northern part, particularly as to the Nor Equatorial Current.

The system of Equatorial Currents in t Pacific Ocean presents more well-defined con tions. The observation material from t Pacific is also more extensive, including as does several sections across the Equator Currents. Therefore, more far-reaching co clusions have to be deferred until the Paci data are discussed.

## References


ɔwes, A. J.
950. An Introduction to the Hydrology of South African Waters. Fisheries a. Marine Biol. Survey Division Invest. Report no. 12.

FANT, A.
936. Die Troposphäre. Deutsche Atlantische Exped. Meteor, 1925—1927, Wiss. Erg., Bd. VI, Teil 1, 3. Lief., p. 289.
941. Die absolute Topographie des physikalischen Meeresniveaus und der Druckflächen, sowie die Wasserbewegungen im Atlantischen Ozean. Deutsche Atlantische Exped. Meteor 1925—1927, Wiss. Erg., Bd. VI, 2 Teil, 5. Lief., p. 191.

LLER, L.
929. Die Zirkulation des Indischen Ozeans. Auf Grund von Temperatur- und Salzgehaltstiefenmessungen und Oberflächenstrombeobachtungen. Berlin Univ., Institut f. Meereskunde, Veröff., N. F., A. Geogr.-naturwiss. Reihe, Heft 21.

NTGOMERY, R. B. and E. PALMÉN.
940. Contribution to the question of the Equatorial Counter Current. Jour. Marine Research, v. 3, p. 112.

PARR, A. E.
1938. On the Validity of the Dynamic Topographic Method for the Determination of Ocean Current Trajectories. Jour. Marine Research v. 1, p. 119.

REID, R. O.
1948. The Equatorial Currents of the Eastern Pacific as maintained by the Stress of the Wind. Journ. Marine Research, v. 7, no. 2, p. 74.

SCHOTT, G.
1935. Geographie des Indischen und Stillen Ozeans. Hamburg, Verlag von C. Boysen.
1943. Weltkarte. Ann. d. Hydrogr. u. Mar. Meteorol. Tafel 22.

SVERDRUP, H. U.
1932. Arbeider i luft- og havsforskning. Chr. Michelsens Institutt for Videnskap og Aandsfrihet, Beretninger, v. 2, no. 5.
1947. Wind-driven currents in a baroclinic ocean with application to the Equatorial Currents of the Eastern Pacific. Proc. Nat. Accad. Sciences, v. 33, no. 11. p. 318.

SVERDRUP, H. U., M. W. JOHNSON and K. H. FLEMING
1942. The Oceans, their Physics, Chemistry and General Biology. New York.